

**Absolute intensities of medium-energy muons in the vertical and at zenith angles 55°–85°**

P. J. Green, N. M. Duller, and C. E. Magnuson\*

*Physics Department, Texas A & M University, College Station, Texas 77843*

L. M. Choate

*Sandia Laboratories, Radiation Physics Division, Albuquerque, New Mexico 87185*W. R. Sheldon, A. R. Osborne,<sup>†</sup> and J. R. Benbrook*Physics Department, University of Houston, Houston, Texas 77004*

M. S. Abdel-Monem

*Physics Department, University of Petroleum and Minerals, Dhahran, Saudi Arabia*

(Received 11 December 1978; revised manuscript received 14 May 1979)

Measurements of absolute differential muon intensities have been made with the Texas A & M–University of Houston solid-iron magnetic spectrometer at axis orientations of 0°, 65°, and 80°. The momentum range covered is from 2 to 300 GeV/c although emphasis has been on the accuracy of measurements from 20 to 50 GeV/c. The large-zenith-angle orientations have allowed measurements of the intensity over the zenithal range 55°–85°. The actual measured intensities are presented along with the final corrected intensities evaluated at standard momenta. These measurements, made with a single instrument, may serve as normalization intensities for large-zenith-angle high-MDM (maximum detectable momentum) spectrometers which cannot be operated at arbitrary axis orientations and for which intensity-normalization points at moderate energies can be useful. The results are shown to be consistent with the most recent measurements from the Kiel-DESY magnetic spectrometer. The procedures for recording and analyzing the data are presented in detail.

**I. INTRODUCTION**

Many measurements of the muon intensity have been made both in the atmosphere and underground with the overall objective of obtaining information on the nature of high-energy interactions as well as on the spectral characteristics of the primary spectrum. Underground measurements can routinely extend the range of measurement upward in energy, but most such measurements have been subject to serious uncertainties in underground depth and fluctuations in the muon interaction with the overburden. A deep-underground experiment which has successfully dealt with these problems is the French-U.S. muon experiment carried out in the Mt. Blanc Tunnel.<sup>1</sup> Ground-level experiments of accuracy comparable with the Mt. Blanc results would provide valuable complementary data to test for corroboration of muon intensity spectral characteristics at high energies and, for the first time, give direct experimental measurements of range vs energy for very-high-energy muons in solid matter. For reasons discussed here, ground-level measurements at high energies are not yet of adequate quality to make these goals fully realizable. Ground-level measurements are limited by the resolution of the spectrometers used and by small apertures. Many surface measurements have been made with solid-iron magnetic spectrometers.

As the measurements were extended up in energy above a few tens of GeV, the spectrometers became necessarily larger and heavier to provide a greater field line integral and to increase the aperture significantly. As measurements were extended to large zenith angles, the data provided by a single instrument were usually over a very narrow range of zenith angle. The result has been that the muon intensity over a wide range of zenith angle even at moderately high energy has not been measured carefully and absolutely with a single instrument. Most high-energy measurements reported thus far have given relative intensities which have necessarily been normalized to available absolute measurements at low energies, and research groups have chosen a variety of normalization points and techniques of normalization. Renormalization of intensities to a common point still leaves spectral discrepancies which frustrate attempts at a firm consensus. Kirillov-Ugryumov *et al.*<sup>2</sup> have noted the astonishing magnitudes of these discrepancies at energies from 10 GeV to 2 TeV even in the vertical intensity measurements. These discrepancies can arise from variations of the efficiencies of instruments both with energy and with zenith angle. Detailed knowledge of these efficiencies is generally unavailable, mainly because an indeterminate bias of data arises from large-scale rejection of complicated events (which can represent as much as

50% of the recorded data at large zenith angles in some previous work).

Our goal has been to measure the muon intensity at a few times ten GeV/ $c$  in the vertical direction and over the zenithal range  $55^\circ$  to  $85^\circ$  with a single instrument. All measurements are absolute with no normalizations and all accumulated data have been accounted for in detail. Our measurements actually extend over the range 2–250 GeV/ $c$ , although our goal of obtaining absolute normalization intensities is attained for the narrower range of 20–50 GeV/ $c$ . Measurements made with the new generation of large high-MDM (maximum detectable momentum) spectrometers can be referenced to these measurements since their results are usually a presentation of relative flux measurements normalized to vertical intensities. The number of large operating spectrometers is currently rather small, but the data of all such spectrometers used now and in the past can be rendered more useful (or corroborated) by the results of the present experiment.

## II. APPARATUS

### A. The AMH magnetic spectrometer

The AMH magnetic spectrometer (Texas A & M and University of Houston collaboration) has been used to measure absolute muon intensities in the vertical direction and over the zenithal range  $55^\circ$ – $85^\circ$  at momenta 2–250 GeV/ $c$ . The AMH spectrometer has been described in detail elsewhere,<sup>3</sup> but here we review essential features of the system for convenient reference and to reinforce the claim that the final results in the range 20–50 GeV/ $c$  are of calibration standard quality at the zenith angles reported. The spectrometer incorporates solid-iron magnets, plastic scintillator primary detectors, and wide-gap optical spark chambers. Muon trajectory information is obtained from photographs taken from orthogonal views of the spark chambers. The magnets, scintillators, spark chambers, cameras, and associated control systems are integrally mounted on large rocker beams to allow rotation of the spectrometer from the vertical to the horizontal, facilitating measurement of intensities with a single instrument over all zenith angles (see Fig. 1).

The magnet sections were made of soft steel laminae slotted in the center to form the equivalent of a rectangular compressed toroid. The long sections of the magnet were wrapped with two 450-turn layers of #14 AWG wire. A magnetizing current of 12 A produces a magnetic field of 18.7 kG in the iron. Search coils included at many points within the volume of the magnet showed the magnetic field

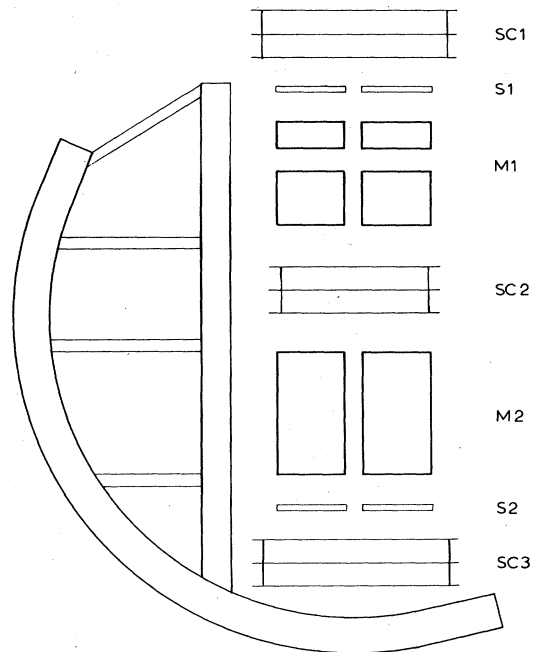


FIG. 1. The AMH spectrometer. SC—wide-gap spark chambers, S—scintillators, M—solid iron magnets. (The dimensions of the apparatus may be determined by scaling from the 58-cm-high M2 magnet.)

to be uniform over the wrapped volume to within 1.5%. The total  $\int B dl$  is 16.3 kG m. During the course of all data accumulation, the polarity of the current was reversed periodically to remove any asymmetries introduced in the data by possible physical dissimilarities between the two sides of the magnets.

A total of three wide-gap spark chambers are located above, below, and between the magnet sections. Each chamber consists of two 10-cm gaps formed by aluminum plates separated by acrylic plastic walls. The chambers are continuously flushed with a helium-isobutane mixture (99.95% He, 0.05% isobutane), and provide essentially 100% efficiency for multiple as well as single tracks. Prompt 100-kV pulses are provided by an eight-stage Marx generator.

The spark chambers are viewed in two orthogonal directions along and perpendicular to the magnetic field direction by two 16-mm cameras. A mirror system allows each camera to record the images of all three spark chambers in a single frame. To compensate for optical distortions, a set of fiducial filaments is strung at one-in intervals in a plane completely across the field of view of each camera spanning all three chambers. The fiducials define a single reference frame for muon trajectory measurements.

### B. Digitizing system

Photographs of the chamber sparks are projected onto a digitizing table for conversion of optical trajectory information to digital form. The table consists of a cursor-tracking unit beneath the surface of the table coupled to  $X$  and  $Y$  axis optical encoders. This system has an  $X, Y$  coordinate reproducibility of 0.1 mm. A front surface cursor is aligned along the projected track and several coordinates recorded to allow fitting of straight lines to track coordinates. Repeated measurements of tracks at various locations in the chambers gave an rms angular-measurement uncertainty of 1.0 mrad and a position uncertainty of 0.4 mm.

### C. Film scanning procedure

Visual examination of the events turned out to be very valuable as an aid to avoid rejection of events which contained a muon but also included other tracks. Several classifications were used to account for all muon events even if there were associated knock-on electrons or if the muon was in a shower. The result was that, of the legitimate events (events having measurable sparks in the upper and lower chambers), only about 3% were actually unanalyzable, whereas over 20% of the events, especially at the larger zenith angles, were complicated by associated knock-on electrons.

### D. Momentum determination

The computer effectively moved the cameras from their finite viewing distance to infinity and reconstructed the sparks in real space. The momentum vector for each particle was then calculated. Events were subsequently examined carefully to ensure that the muon trajectories were within the useful aperture and could not at any point miss some essential component of the spectrometer. The aperture was slightly reduced by computer selection to eliminate edge effects.

## III. CORRECTIONS TO THE MEASURED INTENSITIES

The ratio of the magnetic bending to the rms multiple scattering in the AMH instrument is 5 : 1. This effectively introduces a 20% momentum independent statistically distributed error in the momentum determination. Further noise-type error is introduced by angle and position uncertainties. Given that the rms angular-measurement error is 1.0 mrad, if we consider the momentum to be determined solely from the difference in trajectory angles above and below the magnets, the rms error in angular difference,  $\Delta\theta$ , is

1.4 mrad. Using the normally adopted procedure of calculating the MDM by direct use of  $\Delta\theta_{\text{rms}}$  for muons of infinite momentum, we obtain an MDM of 345 GeV/c. However, the MDM is dramatically increased if all the redundant position and angle information is used. Using maximum-likelihood techniques to find the best-fit trajectory leads to an MDM of nearly 700 GeV/c. The MDM itself is not as important as the more detailed nature of the entire error distribution and the way it is used to relate a measured intensity spectrum to a real spectrum. In most publications, the methods of making resolution corrections are not given. A procedure suggested by Hayman and Wolfendale<sup>4</sup> is frequently referenced. In this procedure, the ratio of the measured to the real spectrum is calculated assuming that the error distribution in the deflection domain is purely Gaussian and that the spectrum follows a power law,  $p^{-3}$ . Most muon spectra can be represented by a fixed power law only over a very limited range of momentum. Large-zenith-angle measurements at low and moderate momenta reveal spectra that are much flatter than a  $p^{-3}$  spectrum. Furthermore, Osborne<sup>5</sup> has noted that a realistic representation of the multiple Coulomb scattering distribution has a much longer "tail" than the simple Gaussian form. Accommodating these factors leads to spectral corrections that are very dependent on the overall shape of the measured spectrum. For this reason we have chosen to report here actual measured intensities and the "best-fit" spectra derived from these measurements, instead of giving intensity measurements corrected point by point for scattering and measurement error. We treat the measured differential spectrum at any given zenith angle as the result of a real spectrum spread by multiple Coulomb scattering and measurement error:

$$i_m(p, \theta) = \int i_r(p', \theta) f_{sc}(p; p') g(p; p') dp', \quad (1)$$

where  $f_{sc}$  is the Coulomb scattering function,  $g$  is the resolution scattering function, and  $i_r$  is the real muon spectrum that we seek. To represent the real intensity we choose the function<sup>6</sup>

$$i_r(p, \theta) = I_0 W_\mu(p, \theta) (p + \Delta p)^{-\gamma_0} \frac{\delta_\pi^{-\gamma_0+1} B_\pi \sec \theta}{B_\pi \sec \theta + (p + \Delta p) \delta_\pi}, \quad (2)$$

where

$I_0$  = normalization constant,

$p$  = the muon momentum at observation,

$\theta$  = the zenith angle at observation,

$\gamma_0$  = the fitted spectral exponent,

$$B_\pi = 117 \text{ GeV}/c,$$

$$\delta_\pi = \left[ \frac{(R^2 - 1)(\gamma_0 + 1)}{R^2(1 - R^{-2(\gamma_0 + 1)})} \right]^{1/\gamma_0},$$

$$R = 1.316 \text{ or } m_\pi/m_\mu,$$

$\Delta p$  = the momentum loss of muons  
from production to sea level

$$= (a + bp)(X_0 - X_p) \sec \theta;$$

$$a = 2.5 \times 10^{-3} (\text{GeV}/c)(\text{g}/\text{cm}^2)^{-1},$$

$$b = 2.5 \times 10^{-6} (\text{g}/\text{cm}^2)^{-1},$$

$X_0$  = atmospheric depth at sea level  
(1033 g/cm<sup>2</sup>),

$X_p$  = mean atmospheric depth at production  
( $\approx 100$  g/cm<sup>2</sup>),

$W_\mu(p, \theta)$  = muon survival probability

$$= \frac{X_p}{X_0} \left( \frac{p}{p + \Delta p_0} \right)^{B_\mu \sec \theta / (p + \Delta p)},$$

$$B_\mu = 1.1192 \text{ GeV}/c,$$

and

$$\Delta p_0 = \frac{X_0 - X_p}{X_0} \Delta p$$

$$= 0.9032 \Delta p.$$

This function represents a phenomenological model which relates physical parameters to an observed spectrum, but we have used it only because it is a two-parameter function that mathematically represents the observed spectra quite well. It allows large-zenith-angle spectra to be quite flat at low momenta and yet become very steep at the higher momenta. Before discussing the final results, one further point concerning resolution corrections should be considered. In examining all the observable input available from the AMH spectrometer, Osborne<sup>5</sup> notes that the measurement error determined by successive remeasurements of tracks on the digitizing table consistently gives an underestimate of the magnitude of the correction to the measured intensity required to yield a true muon intensity. In particular, he has examined the trajectory information obtained in the direction of no magnetic deflection of the muons. To reproduce the scattering distribution observed in the no-deflection direction, he has defined a  $P_{\text{CDM}}$ , or characteristically determined momentum, which is related to resolution corrections very much as the MDM is but which is allowed to be a fitting parameter. He finds that the best-fit  $P_{\text{CDM}}$  is nearer 100 GeV/c for the AMH spectrometer, as compared with an MDM (determined in

the usual manner) of 345 GeV/c. Furthermore, we have found a significant reduction in the  $\chi^2$  of a spectral fit to other spectrometer results when the  $P_{\text{CDM}}$  is allowed to be a fitting parameter and  $P_{\text{CDM}}$  is found to be systematically much lower than the MDM. This point will be discussed in more detail in another paper. Here we wish to suggest that absolute intensity measurements made with magnetic spectrometers may be considered to be accurate up to momenta near one half the MDM, but that above this value it is quite likely that the scattering and resolution corrections have been underestimated and that the final reported intensities are systematically higher than the actual values. The AMH spectrometer is no exception. We find that a  $P_{\text{CDM}}$  of 100 GeV/c gives a much better fit to the high momentum points than a  $P_{\text{MDM}}$  of 345 GeV/c. For this reason we only consider intensities up to 100 GeV/c to be reliable.

#### IV. DISCUSSION OF RESULTS

The aperture of the AMH spectrometer has been discussed in detail elsewhere.<sup>7</sup> The acceptance angle of muons above 10 GeV/c is  $\pm 9^\circ$  in the zenithal coordinate and  $\pm 18^\circ$  in the azimuthal coordinate. The variation of aperture with angle and energy is given in Table I for both the  $65^\circ$  and  $80^\circ$  orientations. At momenta above 10 GeV/c the aperture decreases essentially linearly from a maximum value at the spectrometer axis direction to zero at zenith angles  $9^\circ$  off the axis. Because of the near symmetry of the aperture over the total opening angle of the spectrometer and the smooth variation of the intensity with zenith angle, the average angle is essentially the same as the spectrometer axis tilt angle for the  $55^\circ$ - $75^\circ$  and  $70^\circ$ - $90^\circ$  measured intensities. The lack of symmetry of the aperture in the  $5^\circ$  bins causes the average angles to differ significantly from the midpoints of the zenithal bins.

The intensities at  $0^\circ$ ,  $65^\circ$ , and  $80^\circ$  measured over the entire aperture are given without corrections in Table II. Measured intensities in  $5^\circ$  zenithal bins from  $55^\circ$  to  $90^\circ$  are given in Table III.

The best-fit parameters  $I_0$  and  $\gamma_0$ , which were determined by fitting the corrected measured absolute differential intensities with the two-parameter phenomenological model, are presented in Table IV. Although the function used to fit the data has spectral form which provides excellent fitting, the model is not sufficiently detailed to fit an entire family of curves, so the two-parameter function is used to fit each curve separately. The actual intensities evaluated at standard momenta are listed in Table V. We would reemphasize that these final intensities fit measured re-

TABLE I. The aperture of the spectrometer (in  $\text{cm}^2 \text{sr}$ ) as a function of momentum and zenith angle for the  $65^\circ$  and  $80^\circ$  axis orientations.

Particle momentum (GeV/c)	Acceptance geometry			
	Range of zenith angles for the $65^\circ$ axis orientation			
	$55^\circ-60^\circ$	$60^\circ-65^\circ$	$65^\circ-70^\circ$	$70^\circ-75^\circ$
2.0	29.7	13.2	11.5	28.8
3.5	28.7	51.1	52.4	30.1
5.5	21.8	65.4	67.9	24.6
7.5	18.9	69.7	72.7	22.3
9.5	17.5	71.5	74.8	21.2
15.0	16.1	73.0	76.7	20.0
22.0	15.7	73.5	77.4	19.6
100.0	15.3	73.9	78.0	19.3

Particle momentum (GeV/c)	Acceptance geometry			
	Range of zenith angles for the $80^\circ$ axis orientation			
	$70^\circ-75^\circ$	$75^\circ-80^\circ$	$80^\circ-85^\circ$	$85^\circ-90^\circ$
2.0	29.8	12.5	12.2	28.1
3.5	29.4	51.6	52.3	28.7
5.5	22.7	66.5	67.1	23.2
7.5	19.9	71.0	71.7	21.0
9.5	18.6	72.9	73.5	19.9
15.0	17.2	74.6	75.2	18.8
22.0	16.8	75.2	75.8	18.4
100.0	16.4	75.6	76.2	18.2

sults only after inclusion of the effects of measurement error (maximum-detectable-momentum correction) and multiple Coulomb scattering. This can be seen more clearly in Fig. 2, where the  $0^\circ$ ,  $65^\circ$ , and  $80^\circ$  best-fit intensities are displayed along with measured intensities. In Fig. 3, values of  $p^3 i(p)$  are graphed using the final best-fit real intensities. This graph shows clearly where the  $65^\circ$  and the  $80^\circ$  intensities cross the vertical intensity.

Bahdwar *et al.*<sup>8,9</sup> have calculated the absolute

sea-level muon momentum spectrum using available accelerator data. The very good agreement of their calculations with out absolute measurements has been noted in the vertical<sup>8</sup> and at  $65^\circ$  zenith angle.<sup>9</sup> We emphasize that their calculation is absolute, not normalized.

Values of  $p^3 i(p)$  determined from the best fits for the smaller zenithal bins are shown in Fig. 4, where they are compared with the most recent intensity measurements reported for the Kiel-DESY

TABLE II. The measured differential intensities [in  $\text{cm}^{-2} \text{sr}^{-1} \text{sec}^{-1} (\text{GeV}/c)^{-1}$ ] over the entire aperture of the spectrometer.

Momentum interval (GeV/c)	$0^\circ$ orientation		$65^\circ$ orientation		$80^\circ$ orientation	
	Mean momentum (GeV/c)	Measured intensity	Mean momentum (GeV/c)	Measured intensity	Mean momentum (GeV/c)	Measured intensity
2-4 <sup>a</sup>	2.78	$(9.58 \pm 0.16) \times 10^{-4}$	2.87	$1.27 \pm 0.02 \times 10^{-4}$	2.68	$1.75 \pm 0.06 \times 10^{-5}$
4-7	5.24	$4.00 \pm 0.08 \times 10^{-4}$	5.38	$7.74 \pm 0.14 \times 10^{-5}$	5.40	$1.13 \pm 0.04 \times 10^{-5}$
7-10	8.33	$1.75 \pm 0.06 \times 10^{-4}$	8.34	$4.72 \pm 0.10 \times 10^{-5}$	8.40	$8.71 \pm 0.32 \times 10^{-6}$
10-15	12.18	$8.33 \pm 0.30 \times 10^{-5}$	12.32	$2.86 \pm 0.06 \times 10^{-5}$	12.36	$6.38 \pm 0.21 \times 10^{-6}$
15-25	19.20	$2.96 \pm 0.12 \times 10^{-5}$	19.62	$1.28 \pm 0.03 \times 10^{-5}$	19.68	$4.06 \pm 0.12 \times 10^{-6}$
25-40	31.40	$8.14 \pm 0.50 \times 10^{-6}$	31.60	$4.52 \pm 0.15 \times 10^{-6}$	31.70	$1.79 \pm 0.66 \times 10^{-6}$
40-70	52.40	$1.77 \pm 0.16 \times 10^{-6}$	52.42	$1.45 \pm 0.06 \times 10^{-6}$	52.60	$6.78 \pm 0.30 \times 10^{-7}$
70-110	87.10	$4.79 \pm 0.78 \times 10^{-7}$	87.20	$4.66 \pm 0.38 \times 10^{-7}$	87.40	$2.46 \pm 0.16 \times 10^{-7}$
110-700	249.90	$3.95 \pm 0.53 \times 10^{-8}$	251.1	$4.38 \pm 0.39 \times 10^{-8}$	251.1	$2.92 \pm 0.17 \times 10^{-8}$

<sup>a</sup> 1.6-4 for the  $80^\circ$  orientation.

TABLE III. The measured differential intensities [in  $\text{cm}^{-2} \text{sr}^{-1} \text{sec}^{-1} (\text{GeV}/c)^{-1}$ ] in  $5^\circ$  zenithal bins.

Momentum (GeV/c)	65° orientation				65° and 80°	
	55°-60° $\bar{\theta} = 58.6^\circ$	60°-65° $\bar{\theta} = 63.0^\circ$	65°-70° $\bar{\theta} = 67.0^\circ$	65°-70° $\bar{\theta} = 67.0^\circ$	70°-75° $\bar{\theta} = 72.5^\circ$	70°-75° $\bar{\theta} = 72.5^\circ$
2.87 <sup>a</sup>	$(2.70 \pm 0.08) \times 10^{-4}$	$1.36 \pm 0.05 \times 10^{-4}$	$6.65 \pm 0.32 \times 10^{-5}$	$6.65 \pm 0.32 \times 10^{-5}$	$4.85 \pm 0.27 \times 10^{-5}$	$4.85 \pm 0.27 \times 10^{-5}$
5.40	$1.47 \pm 0.05 \times 10^{-4}$	$9.38 \pm 0.25 \times 10^{-5}$	$5.33 \pm 0.18 \times 10^{-5}$	$5.33 \pm 0.18 \times 10^{-5}$	$3.09 \pm 0.20 \times 10^{-5}$	$3.09 \pm 0.20 \times 10^{-5}$
8.40	$7.55 \pm 0.42 \times 10^{-5}$	$5.80 \pm 0.19 \times 10^{-5}$	$3.55 \pm 0.14 \times 10^{-5}$	$3.55 \pm 0.14 \times 10^{-5}$	$2.29 \pm 0.18 \times 10^{-5}$	$2.29 \pm 0.18 \times 10^{-5}$
12.36	$4.24 \pm 0.26 \times 10^{-5}$	$3.42 \pm 0.11 \times 10^{-5}$	$2.31 \pm 0.09 \times 10^{-5}$	$2.31 \pm 0.09 \times 10^{-5}$	$1.39 \pm 0.11 \times 10^{-5}$	$1.39 \pm 0.11 \times 10^{-5}$
19.68	$1.46 \pm 0.11 \times 10^{-5}$	$1.51 \pm 0.05 \times 10^{-5}$	$1.16 \pm 0.04 \times 10^{-5}$	$1.16 \pm 0.04 \times 10^{-5}$	$6.56 \pm 0.56 \times 10^{-6}$	$6.56 \pm 0.56 \times 10^{-6}$
31.70	$4.82 \pm 0.53 \times 10^{-6}$	$5.15 \pm 0.25 \times 10^{-6}$	$4.10 \pm 0.22 \times 10^{-6}$	$4.10 \pm 0.22 \times 10^{-6}$	$2.82 \pm 0.32 \times 10^{-6}$	$2.82 \pm 0.32 \times 10^{-6}$
52.60	$1.68 \pm 0.28 \times 10^{-6}$	$1.53 \pm 0.10 \times 10^{-6}$	$1.46 \pm 0.10 \times 10^{-6}$	$1.46 \pm 0.10 \times 10^{-6}$	$8.79 \pm 1.3 \times 10^{-7}$	$8.79 \pm 1.3 \times 10^{-7}$
87.40	$4.05 \pm 1.1 \times 10^{-7}$	$4.34 \pm 0.52 \times 10^{-7}$	$5.40 \pm 0.69 \times 10^{-7}$	$5.40 \pm 0.69 \times 10^{-7}$	$2.75 \pm 0.62 \times 10^{-7}$	$2.75 \pm 0.62 \times 10^{-7}$
251.1	$5.02 \pm 1.3 \times 10^{-8}$	$4.10 \pm 0.51 \times 10^{-8}$	$5.04 \pm 0.80 \times 10^{-8}$	$5.04 \pm 0.80 \times 10^{-8}$	$3.09 \pm 1.1 \times 10^{-8}$	$3.09 \pm 1.1 \times 10^{-8}$
		80° orientation				
	75°-80° $\bar{\theta} = 78.0^\circ$	80°-85° $\bar{\theta} = 82.0^\circ$	85°-90° $\bar{\theta} = 86.5^\circ$			
2.68	$1.61 \pm 0.11 \times 10^{-5}$	$4.66 \pm 0.61 \times 10^{-6}$	$3.85 \pm 1.9 \times 10^{-6}$	$3.85 \pm 1.9 \times 10^{-6}$		
5.40	$1.40 \pm 0.07 \times 10^{-5}$	$4.26 \pm 0.37 \times 10^{-6}$	$1.12 \pm 0.31 \times 10^{-6}$	$1.12 \pm 0.31 \times 10^{-6}$		
8.40	$1.19 \pm 0.06 \times 10^{-5}$	$3.53 \pm 0.33 \times 10^{-6}$	$1.07 \pm 0.34 \times 10^{-6}$	$1.07 \pm 0.34 \times 10^{-6}$		
12.36	$9.23 \pm 0.41 \times 10^{-6}$	$3.03 \pm 0.23 \times 10^{-6}$	$7.71 \pm 2.3 \times 10^{-7}$	$7.71 \pm 2.3 \times 10^{-7}$		
19.68	$5.92 \pm 0.23 \times 10^{-6}$	$2.36 \pm 0.15 \times 10^{-6}$	$3.50 \pm 1.1 \times 10^{-7}$	$3.50 \pm 1.1 \times 10^{-7}$		
31.70	$2.35 \pm 0.12 \times 10^{-6}$	$1.28 \pm 0.09 \times 10^{-6}$	$5.91 \pm 3.1 \times 10^{-7}$	$5.91 \pm 3.1 \times 10^{-7}$		
52.60	$8.27 \pm 0.52 \times 10^{-7}$	$5.53 \pm 0.42 \times 10^{-7}$	$2.77 \pm 0.61 \times 10^{-7}$	$2.77 \pm 0.61 \times 10^{-7}$		
87.40	$3.04 \pm 0.28 \times 10^{-7}$	$2.09 \pm 0.22 \times 10^{-7}$	$4.96 \pm 2.3 \times 10^{-8}$	$4.96 \pm 2.3 \times 10^{-8}$		
251.1	$3.60 \pm 0.28 \times 10^{-8}$	$2.65 \pm 0.26 \times 10^{-8}$	$9.95 \pm 3.2 \times 10^{-9}$	$9.95 \pm 3.2 \times 10^{-9}$		

<sup>a</sup> 2.77 for  $\bar{\theta} = 72.5^\circ$ .

air-gap spectrometer.<sup>10</sup> The largest-zenith-angle Kiel intensities date back to an earlier measurement.<sup>11</sup> It can be seen that the results are in very good agreement for momenta up to about 50 GeV/c. The intensity is decreasing dramatically with zenith angle below 50 GeV/c. For this reason, the  $81^\circ$  measurements from Kiel are in excellent agreement with our  $82^\circ$  best fit when we note the position of the  $81^\circ$  points between the  $78^\circ$  and  $82^\circ$

TABLE IV. Parameters for best fit of intensity model to data after inclusion of multiple Coulomb scattering and resolution effects. Units are such that  $i_r$  is in  $\text{cm}^{-2} \text{sr}^{-1} \text{sec}^{-1} (\text{GeV}/c)^{-1}$  and  $p$  is in GeV/c [see Eq. (2)].

Range of zenith angles	Normalization parameter ( $I_0$ )	Spectral parameter ( $\gamma_0$ )
0° overall	0.2535	2.743
65° overall	0.1200	2.603
80° overall	0.0940	2.606
55°-60°	0.2042	2.749
60°-65°	0.1602	2.664
65°-70°	0.0676	2.461
70°-75°	0.0957	2.637
75°-80°	0.1077	2.615
80°-85°	0.0361	2.413
85°-90°	0.2031	2.831

curves. The actual average  $\theta$  for the Kiel  $85^\circ$ - $87.5^\circ$  measurement is not reported, but it is probably slightly less than  $86^\circ$ . Consequently the Kiel large-angle measurement is in good agreement with our  $86.5^\circ$  curve. Systematic deviations occur at the high energies. We have reason to believe that these differences arise because of different procedures used for making the resolution correction to the data.

The most recent reported spectrometer measurements are from Kellogg *et al.*<sup>12</sup> They measured absolute integral and differential intensities at  $30^\circ$  and  $75^\circ$  with a magnetic spectrometer whose MDM was assumed to be at least 1200 GeV/c. They used a momentum selector which gave a half efficiency momentum of 50 GeV/c. We have included their measurements at  $75^\circ$  on the  $p^3 i(p)$  plot for comparison. The intensities over the entire range of overlap are parallel to, but larger than, our final best fit to our  $72.5^\circ$  measurements. We would expect their spectrum to possibly cross our  $72.5^\circ$  result but we would also expect the intensity at 55.6 GeV/c to be noticeably lower than our  $72.5^\circ$  result. Three factors could explain the discrepancy apparent in Fig. 4. First of all, they indicate a  $\pm 5.2\%$  normalization error for their entire set of  $75^\circ$  measurements. Second, the cor-

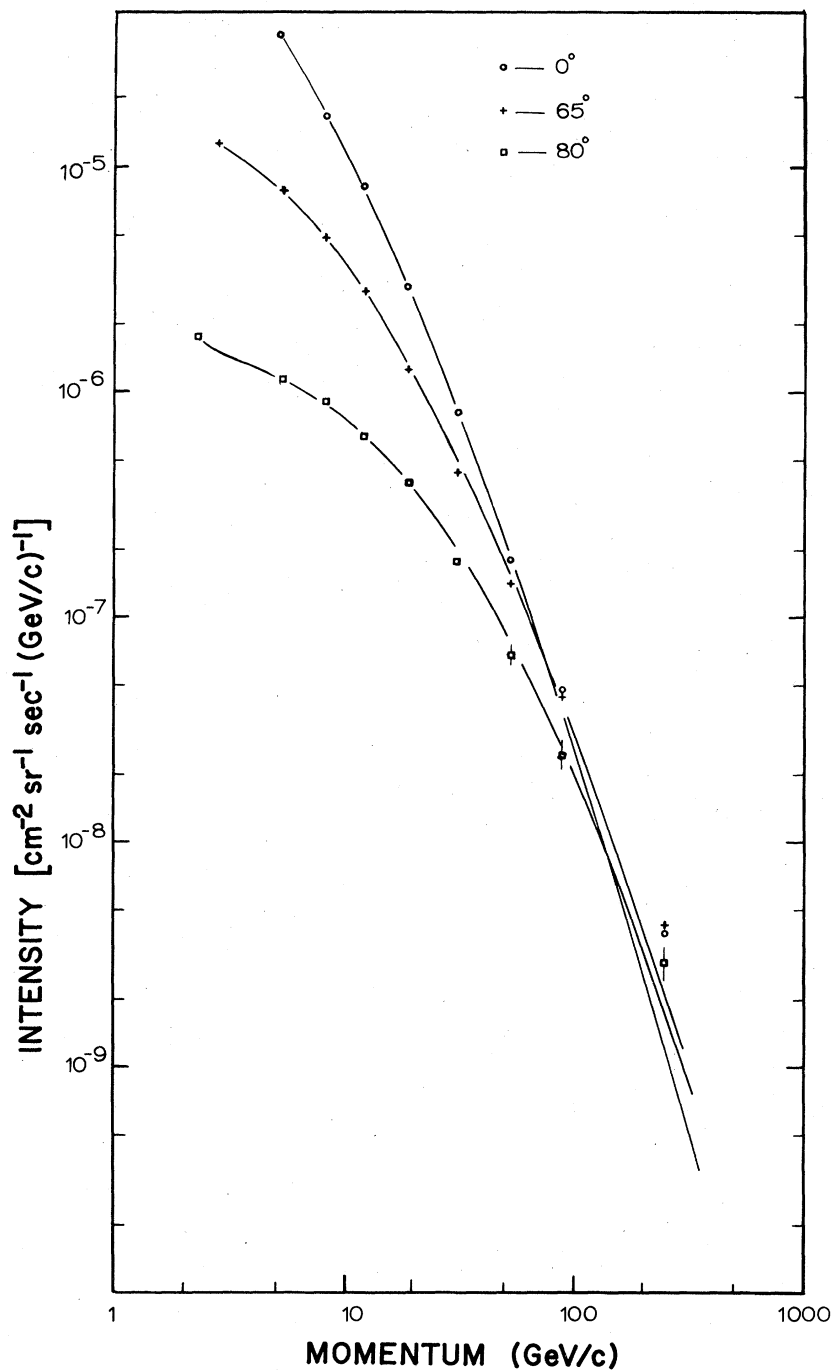


FIG. 2. Measured differential muon intensity at  $0^\circ$ ,  $65^\circ$ , and  $80^\circ$  along with best-fit curves corrected for multiple Coulomb scattering in the iron and for measurement error.

rection factors introduced at their low momentum end to accommodate the momentum selector with a varying efficiency near threshold could have caused the lowest two reported differential intensities to be too high. Finally, our  $72.5^\circ$  curve is derived from data accumulated at spectrometer

orientations of  $65^\circ$  and  $80^\circ$ . The  $72.5^\circ$  overlap region is in a narrow portion of the instrument aperture from both orientations and consequently the statistical uncertainties of these data, especially at the higher momenta, are larger than for any other fitted curve. We have previously commented

TABLE V. Intensities [in  $\text{cm}^{-2} \text{sr}^{-1} \text{sec}^{-1} (\text{GeV}/c)^{-1}$ ] calculated at several zenith angles using the Fyodorov model with the parameters in Table IV.

Momentum (GeV/c)	0.0°	58.0°	63.0°	67.0°
2	$1.35 \times 10^{-3}$	$2.63 \times 10^{-4}$	$1.69 \times 10^{-4}$	$7.73 \times 10^{-5}$
3	$9.09 \times 10^{-4}$	$2.19 \times 10^{-4}$	$1.49 \times 10^{-4}$	$7.27 \times 10^{-5}$
5	$4.50 \times 10^{-4}$	$1.44 \times 10^{-4}$	$1.07 \times 10^{-4}$	$5.77 \times 10^{-5}$
7	$2.51 \times 10^{-4}$	$9.66 \times 10^{-5}$	$7.58 \times 10^{-5}$	$4.44 \times 10^{-5}$
10	$1.23 \times 10^{-4}$	$5.66 \times 10^{-5}$	$4.75 \times 10^{-5}$	$3.04 \times 10^{-5}$
20	$2.46 \times 10^{-5}$	$1.50 \times 10^{-5}$	$1.42 \times 10^{-5}$	$1.09 \times 10^{-5}$
30	$8.53 \times 10^{-6}$	$5.93 \times 10^{-6}$	$6.02 \times 10^{-6}$	$5.12 \times 10^{-6}$
50	$2.03 \times 10^{-6}$	$1.63 \times 10^{-6}$	$1.79 \times 10^{-6}$	$1.73 \times 10^{-6}$
70	$7.45 \times 10^{-7}$	$6.50 \times 10^{-7}$	$7.49 \times 10^{-7}$	$7.89 \times 10^{-7}$
100	$2.46 \times 10^{-7}$	$2.33 \times 10^{-7}$	$2.83 \times 10^{-7}$	$3.26 \times 10^{-7}$
200	$2.55 \times 10^{-8}$	$2.78 \times 10^{-8}$	$3.71 \times 10^{-8}$	$5.08 \times 10^{-8}$
300	$6.35 \times 10^{-9}$	$7.42 \times 10^{-9}$	$1.04 \times 10^{-8}$	$1.58 \times 10^{-8}$
	72.5°	78.0°	82.0°	86.5°
2	$3.68 \times 10^{-5}$	$1.59 \times 10^{-5}$	$3.18 \times 10^{-6}$	$3.51 \times 10^{-7}$
3	$3.60 \times 10^{-5}$	$1.67 \times 10^{-5}$	$3.55 \times 10^{-6}$	$4.10 \times 10^{-7}$
5	$3.04 \times 10^{-5}$	$1.59 \times 10^{-5}$	$3.80 \times 10^{-6}$	$4.79 \times 10^{-7}$
7	$2.44 \times 10^{-5}$	$1.40 \times 10^{-5}$	$3.72 \times 10^{-6}$	$5.12 \times 10^{-7}$
10	$1.75 \times 10^{-5}$	$1.12 \times 10^{-5}$	$3.39 \times 10^{-6}$	$5.25 \times 10^{-7}$
20	$6.65 \times 10^{-6}$	$5.36 \times 10^{-6}$	$2.18 \times 10^{-6}$	$4.52 \times 10^{-7}$
30	$3.17 \times 10^{-6}$	$2.88 \times 10^{-6}$	$1.41 \times 10^{-6}$	$3.53 \times 10^{-7}$
50	$1.07 \times 10^{-6}$	$1.11 \times 10^{-6}$	$6.75 \times 10^{-7}$	$2.11 \times 10^{-7}$
70	$4.83 \times 10^{-7}$	$5.38 \times 10^{-7}$	$3.77 \times 10^{-7}$	$1.32 \times 10^{-7}$
100	$1.96 \times 10^{-7}$	$2.34 \times 10^{-7}$	$1.88 \times 10^{-7}$	$7.19 \times 10^{-8}$
200	$2.92 \times 10^{-8}$	$3.92 \times 10^{-8}$	$4.05 \times 10^{-8}$	$1.67 \times 10^{-8}$
300	$8.79 \times 10^{-9}$	$1.26 \times 10^{-8}$	$1.50 \times 10^{-8}$	$6.18 \times 10^{-9}$

that the procedures for making resolution or MDM corrections to data vary widely among research groups and can lead to significant differences in reported results. However, we do not feel that the Kellogg *et al.* measurements would be significantly affected in this overlap range of 55.9 to 222.6 GeV/c if their MDM is even close to 1200 GeV/c. Their data coincide at 55.6 GeV/c with the Kiel-DESY result at 77° but tend to flatten at the higher momenta. This is consistent with our earlier speculation that the resolution corrections to the Kiel-DESY data have been somewhat underestimated owing to some overestimate of the MDM. We should note the important fact that our spectrometer and the Kellogg *et al.* spectrometer use solid-iron magnets, whereas the Kiel-DESY spectrometer uses an air-gap magnet.

A comparison of our vertical measurement with that from the Magnetic Automated Research Spectrograph (MARS) instrument<sup>13</sup> shows excellent agreement in the region of 20 GeV/c. However, the trend of our results is to become systematically lower than the MARS measurements with increasing energy, differing by 20% at 100 GeV/c. We have previously noted that the resolution correc-

tion to our data is based on a conservative characteristically determined momentum of 100 GeV/c. The MDM of our instrument based on knowledge of our error distribution alone is 345 GeV/c. If this MDM is used in the spectral adjustment of our data, the net result is that the corrected vertical

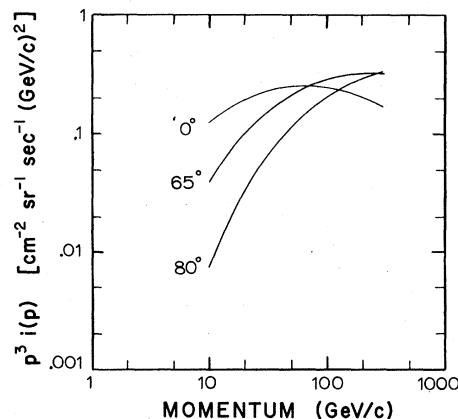


FIG. 3. Plot of  $p^3 i(p)$  versus  $p$  for the best fit differential intensity spectra.



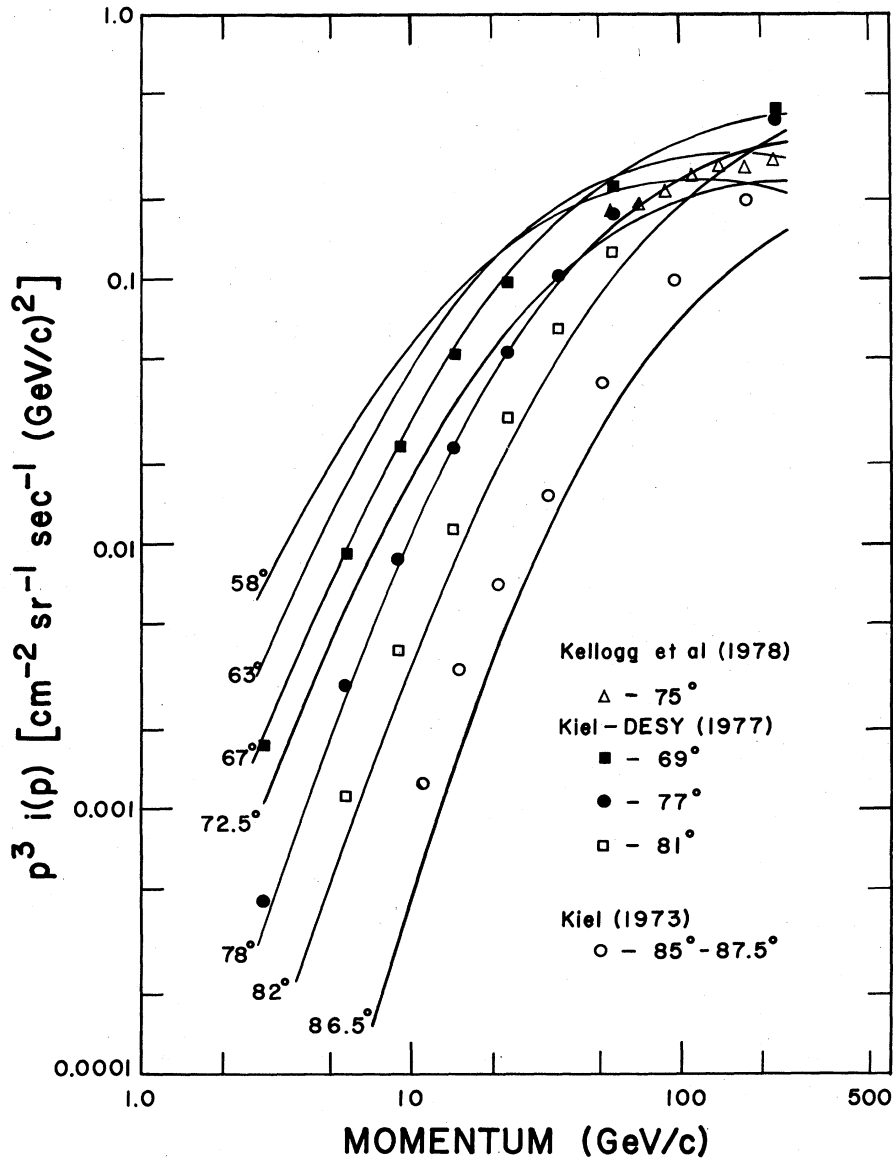


FIG. 4. Comparison of the best fit curves of the present work with the large-zenith-angle measurements of other workers.

intensity of the present experiment becomes flatter and agrees with the MARS result up to 100 GeV/c within 5%. We resist the temptation to use the larger MDM for our spectrometer and thus remove the discrepancy. We prefer the self-consistent use of the characteristically determined momentum, which takes account of the measured scattering in the field of view orthogonal to the muon magnetic deflection view in addition to deflection measurement error. We do not imply that the MARS group has overestimated their MDM by using the value 670 GeV/c. Even if this were an overestimate by a factor of 2, it would make little

difference in the magnitude of the resolution correction at 100 GeV/c.

Burnett *et al.*<sup>14</sup> measured muon intensities in the vertical and at zenith angles from 30° to 82° with a rotatable spectrometer whose derived maximum detectable momentum was 2.5 TeV/c. However, their results vary drastically from any current intensity measurements made at large zenith angles in the range 20–100 GeV/c. In fact, the Durham group<sup>13</sup> found it necessary to raise the Burnett *et al.* vertical intensities by 23% to allow spectral comparison with the MARS vertical measurements. These discrepancies should not be

surprising. Their measurements were not made to provide detailed absolute muon intensities but to search for evidence of muon isotropy at large zenith angles and ultrahigh energies.

#### V. CONCLUSIONS

The main objective of this research was to establish normalization intensities at various large zenith angles near 20 GeV/c. We have made measurements with the spectrometer aligned in the vertical direction and at 65° and 80° zenith angle. These measurements were made with a single instrument and are absolute. We have indicated the procedures used to ensure accuracy of the

reported intensities below 50 GeV/c. The agreement with certain other large-zenith-angle measurements is very good. We should also note that the agreement with the data from the Kiel-DESY spectrometer is particularly significant because their spectrometer is an air-gap magnet system whereas our system utilizes solid-iron magnets. This agreement would indicate that our treatment of the effects of multiple Coulomb scattering in the iron is accurate.

#### ACKNOWLEDGMENTS

This work was supported by NSF Grant No. PHY74-19074A01 and the Research Corporation.

\*Present address: Biosystems Engineering, Texas A & M University, College Station, Texas 77843.

†Present address: Exxon Production Research, Houston, Texas 77001.

<sup>1</sup>W. R. Sheldon, J. R. Benbrook, N. M. Duller, W. G. Cantrell, A. R. Bazer-Bachi, Gilbert Vedremme, and Claude Dunet, *Phys. Rev. D* **17**, 114 (1978).

<sup>2</sup>V. G. Kirillov-Ugryumov, A. A. Petrukhin, and V. V. Shestakov, in *Proceedings of the Fourteenth International Conference on Cosmic Rays, Munich, 1975*, edited by Klaus Pinkau (Max-Planck-Institut, Munich, 1975), Vol. 6, p. 1943.

<sup>3</sup>W. G. Cantrell, N. M. Duller, P. J. Green, J. R. Benbrook, A. R. Osborne and W. R. Sheldon, in *Proceedings of the Thirteenth International Conference on Cosmic Rays, Denver, 1973* (Colorado Associated University Press, Boulder, 1973), Vol. 4, p. 2968.

<sup>4</sup>P. J. Hayman and A. W. Wolfendale, *Proc. Phys. Soc.* **80**, 710 (1962).

<sup>5</sup>A. R. Osborne, dissertation, University of Houston, 1974 (unpublished).

<sup>6</sup>V. M. Fyodorov and Y. A. Trubkin, Academy of Sciences of the USSR, P. N. Lebedev Physical Institute Report No. 175, Moscow, 1973 (unpublished).

<sup>7</sup>P. J. Green, T. A. Nagy, and C. E. Magnuson, *Nucl. Instrum. Methods*, **113**, 241 (1973).

<sup>8</sup>G. D. Bhadwar, S. A. Stephens, and R. L. Golden, *Phys. Rev. D* **15**, 820 (1977).

<sup>9</sup>G. D. Bhadwar and S. A. Stephens, in *Proceedings of the Fifteenth International Conference on Cosmic Rays, Plovdiv, 1977*, edited by B. Betev (Bulgarian Academy of Sciences, Sofia, 1977), Vol. 6, p. 200.

<sup>10</sup>O. C. Allkofer, K. Carstensen, W. D. Dau, H. Jokisch, and H. J. Meyer, in *Proceedings of the Fifteenth International Conference on Cosmic Rays, Plovdiv, 1977*, edited by B. Betev (Bulgarian Academy of Sciences, Sofia, 1977), Vol. 6, p. 38, and private communication.

<sup>11</sup>O. C. Allkofer, K. Carstensen, W. D. Dau, E. Fahnders, and R. Sobania, in *Proceedings of the Thirteenth International Conference on Cosmic Rays, Denver, 1973* (Colorado Associated University Press, Boulder, 1973), Vol. 3, p. 1748.

<sup>12</sup>R. G. Kellogg, H. Kasha, and R. C. Larsen, *Phys. Rev. D* **17**, 98 (1978).

<sup>13</sup>C. A. Ayre, J. M. Baxendale, C. J. Hume, B. C. Nandi, M. G. Thompson, and M. R. Whalley, *J. Phys. G: Nucl. Phys.* **1**, 584 (1975).

<sup>14</sup>T. H. Burnett, G. E. Masek, T. Maung, E. S. Miller, H. Ruderman, and W. Vernon, in *Proceedings of the Thirteenth International Conference on Cosmic Rays, Denver, 1973* (Colorado Associated University Press, Boulder, 1973), Vol. 3, p. 1764.